Catalysis Today 150 (2010) 133–139

Contents lists available at ScienceDirect

Catalysis Today

journal homepage: www.elsevier.com/locate/cattod

High surface-to-volume hybrid platelet reactor filled with catalytically grown vertically aligned carbon nanotubes

Yu Liu [a], Izabela Janowska [a,*], Thierry Romero [a], David Edouard [a], Lâm D. Nguyen [b], Ovidiu Ersen [c], Valérie Keller [a], Nicolas Keller [a], Cuong Pham-Huu [a,*]

[a] Laboratoire des Matériaux, Surfaces et Procédés pour la Catalyse, CNRS-Université de Strasbourg (UDS), UMR 7515 CNRS, 25, rue Becquerel, 67087 Strasbourg Cedex 08, France
[b] Da-Nang University of Technology, University of Da-Nang, 54, Nguyen Luong Bang, Da-Nang, Viet Nam
[c] Institut de Physique et Chimie des Matériaux de Strasbourg CNRS-Université de Strasbourg (UDS), UMR 7504 CNRS, 23, rue du Loess, 67037 Strasbourg Cedex 02, France

ARTICLE INFO

Article history:
Available online 24 October 2009

Keywords:
Microreactor
Aligned carbon nanotubes
Catalysis

ABSTRACT

During the last decade, microstructured reactors have received an impressive development in several fields of applications, especially in the field of catalysis where heat and mass transfers need to be improved. These reactors are generally consisting in sub-millimeter channels which exhibit an extremely high surface-to-volume ratios, typically in the range of 10,000–50,000 $m^2\,m^{-3}$ compared to those of conventional reactors which lie between 100 and 1000 $m^2\,m^{-3}$. In the present work we report the use of extremely high aspect ratio vertically aligned carbon nanotubes (VA-CNTs) which can be efficiently employed as a high surface-to-volume building-block for the platelet hybrid microstructured reactors. Due to the nanoscopic size of the filling material, such reactor displays an extremely high surface-to-volume ratio, expressed in terms of effective surface area along with an affordable pressure drop across the reactor. The assembly mode also allows the easy control (preparation and characterizations) and replacement of the catalyst, in case of deactivation or plugging, which is not a case for the traditional microstructured reactors.

1. Introduction

Microstructured reactors have received during the last decade an impressive development in several fields of application [1,2]. Microstructured reactors are generally consisting in sub-millimeter channels which exhibit an extremely high surface-to-volume ratio, typically in the range of 10,000 to 50,000 $m^2\,m^{-3}$ compared to those of conventional reactors which lie between 100 and 1000 $m^2\,m^{-3}$ [3]. Such high surface-to-volume (S/V) ratio allows the microstructured reactors to be rapidly heated up or cooled down which is not the case of conventional reactors. The high S/V ratio also strongly improves the heat and mass transfers which are key issues for most of the chemical reactions. Microstructured reactors also offer efficient control of the reaction conditions due to the small hold-up, of either reactants or products, which allows the partial or total elimination of hot spots by avoiding thermal runaway, laminar flow behaviour, compactness and parallel processibility. However, immobilization of the catalysts in such small channels, i.e. sub-millimeter dimensions, and a strong anchorage of the catalytic layer on the reactor wall are still difficult to be achieved. In liquid-phase operation, the catalysts are quite often flowed through the microchannel reactor with reactant solutions [4]. The microstructured reactors should also be cheap, easy to build, have a high chemical inertness and a high mechanical strength along with body integrity which allow the easy recovery of both the active phase and the support. Up to now, the machining of these sub-millimeter channels is not straightforward and generally, lithography or other high-tech technologies are needed to ensure the realization of these sub-millimeter channels. The catalyst deposition and recovery also represent problems that need to be addressed.

Regarding the different drawbacks described above, attempts were made to elaborate hybrid microreactors in which the channel is filled with host structures such as metallic or ceramic foams, pure or covered with a network of nanostructured carbon [5–9]. The high porosity of the foam structure ensures the good and homogeneous mixing of the reactants which provide high reaction rate. The high open porosity of the foam structure also allows working at high space velocity without detrimental pressure drop across the reactor channel. The surface-to-volume ratio of these systems is relatively high compared to that of the pristine channel, but still lower than the one offered by micrometer channel

* Corresponding authors. Tel.: +33 3 90 24 26 75; fax: +33 3 90 24 26 74.
E-mail addresses: Izabela.Janowska@ecpm.u-strasbg.fr (I. Janowska), cuong.lcmc@ecpm.u-strasbg.fr (C. Pham-Huu).

0920-5861/$ – see front matter © 2009 Elsevier B.V. All rights reserved.
doi:10.1016/j.cattod.2009.09.007

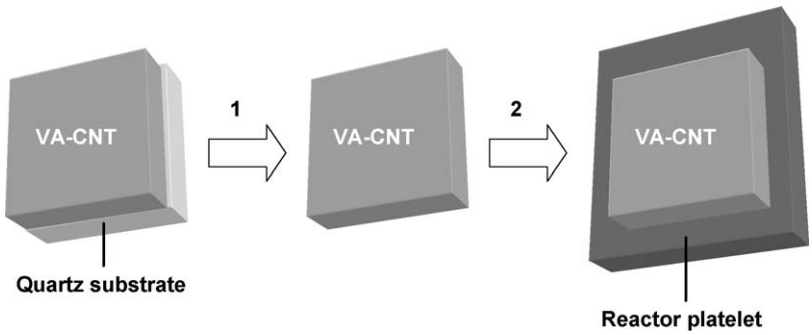

Fig. 1. Schematic representation of the different preparation steps, from the VA-CNTs synthesis to the platelet hybrid reactor, filled with a plate of VA-CNTs. (1) Aqua regia treatment at 80 °C to remove the iron catalyst of the outer surface of the carbon nanotubes. The treatment also allows the removal of the VA-CNTs platelet from the growth quartz substrate. (2) Transfer of the VA-CNTs platelet to the reactor channel.

reactors. Consequently, it is of interest to develop new structured reactors which combine the advantages cited above with a higher surface-to-volume ratio.

Carbon nanotubes, a one-dimensional carbon material with high aspect ratio (the aspect ratio is defined as the length of the major axis divided by the width or diameter of the minor axis), have received an overincreasing scientific interest during the last decades due to their exceptional physical and chemical properties [10–12]. Apart from the field of electronics application, recent works have pointed out the possible use of carbon nanotubes, either pure or doped, as catalyst support in several potential reactions [10–14]. Recently, some attempts to prepare structured catalytic layers based on vertically aligned CNT have been reported [15,16]. Such structured catalyst support allows the development of 3D ordered nanomaterials for several catalytic applications, i.e. 3D ordered PEMFC [17] and 3D catalyst for fine chemical reactions [18].

In the present work we report the use of extremely high aspect ratio vertically aligned carbon nanotubes (VA-CNTs), obtained via catalytic route, which can be efficiently employed as a high surface-to-volume building-block for the elaboration of platelet hybrid microstructured reactors. This new type of support could represent a new alternative to make high surface-to-volume hybrid reactor or mixer with simple building blocks. The support will be integrated into a millimeter plate reactor with a thickness not exceeding few millimeters which generates high heat and mass transfers [19]. The macroscale of the system is related to a LEGO® building approach, which each building unit can be considered as a single reactor while for the scale-up several single units can be assembled in order to meet the required production. Ishigami et al. [20] have reported a similar process based on the combinated use of VA-CNTs and micrometer channel for hydrogenation reaction. However, the microreactor channel in Ishigami's work was not completely filled with VA-CNTs and thus, preferential flow could happen during the reaction. In addition, in this work the VA-CNTs were directly fixed on the microreactor surface and thus, prevent catalyst replacement and control during the impregnation step.

2. Experimental

2.1. Vertically aligned carbon nanotubes (VA-CNTs) synthesis

The VA-CNTs were synthesised *ex situ* by passing a mixture of $Fe(C_5H_5)_2/C_7H_8$ (ferrocene concentration in the toluene solution was fixed at 20 g L^{-1}) over a quartz substrate localized inside a quartz tubular reactor (46 mm diameter, 200 mm length and 1 mm wall thickness) at 850 °C [21–24]. The liquid mixture was injected into the hot zone of a tubular electrical furnace by flowing argon (1.5 L min^{-1}). In order to remove detrimental grease traces and other contaminants, the quartz substrate was cleaned before synthesis by HCl acidic treatment followed by sonication in an ethanolic solution for 30 min. After the synthesis, the substrate with VA-CNTs was cooled down under argon flow to room temperature before discharging. The VA-CNTs were removed from the quartz substrate by an *aqua regia* treatment at 80 °C along with the removal of the residual iron catalyst which was present on the outer surface of the nanotubes. The resulting VA-CNT carpet was washed several times with high purity Elga water (18 MΩ cm, <3 ppm TOC) until a neutral pH was reached. The solid was allowed to dry at 110 °C overnight before use. For the sake of clarity the schematic representation of the different states of the preparation is depicted in Fig. 1.

2.2. Characterization techniques

The specific surface area of the different samples was measured by the BET method using N_2 as adsorbent at liquid nitrogen temperature (TriStar sorptometer). Before measurement, the samples were outgassed at 200 °C overnight in order to desorb moisture and impurities on its surface. The XPS measurements of the support were performed on a MULTILAB 2000 (THERMO VG) spectrometer equipped with Al Kα anode ($h\nu$ = 1486.6 eV) with 10 min of aquisition. Peak deconvolution has been made with "Avantage" program from Thermoelectron Company. The C_{1s} peak at 284.2 eV was used to correct charging effects. Shirley backgrounds were substracted from the raw data to obtain the areas of the C_{1s} peak.

The gross morphology of the carbon and ceramic materials was observed by scanning electron microscopy (SEM) on a Jeol F-6700 FEG with a lattice resolution 1 nm, at accelerating voltage 10 kV. The sample was covered by a thin layer of gold in order to decrease the problem of charge during the analysis. Transmission electron microscopy (TEM) observations were conducted on a Topcon 002-B UHR microscope working at 200 kV accelerated voltage with a point-to-point resolution of 0.17 nm. The sample was sonicated in an ethanol solution and a drop was deposited onto a copper grid covered with a holey carbon membrane for observation.

Thermal gravimetry analysis (TGA) was performed on a Setaram apparatus with an air flow rate of 5 cc min^{-1} and a heating rate of 2 °C min^{-1} from room temperature to 1000 °C. The pressure drop across the reactor was measured by passing a flow of air through the reactor packing at different linear space velocities (0.5–3 m s^{-1}). Pressure drop was measured by a differential captor.

3. Results and discussion

The resulting material from the catalytic CVD growth using a mixture of $Fe(C_5H_5)_2$ and C_7H_8 on a quartz substrate for 3 h is a carpet of VA-CNTs with an average diameter of ca. 100 nm and length greater than 2 mm giving an aspect ratio of ca. 20,000

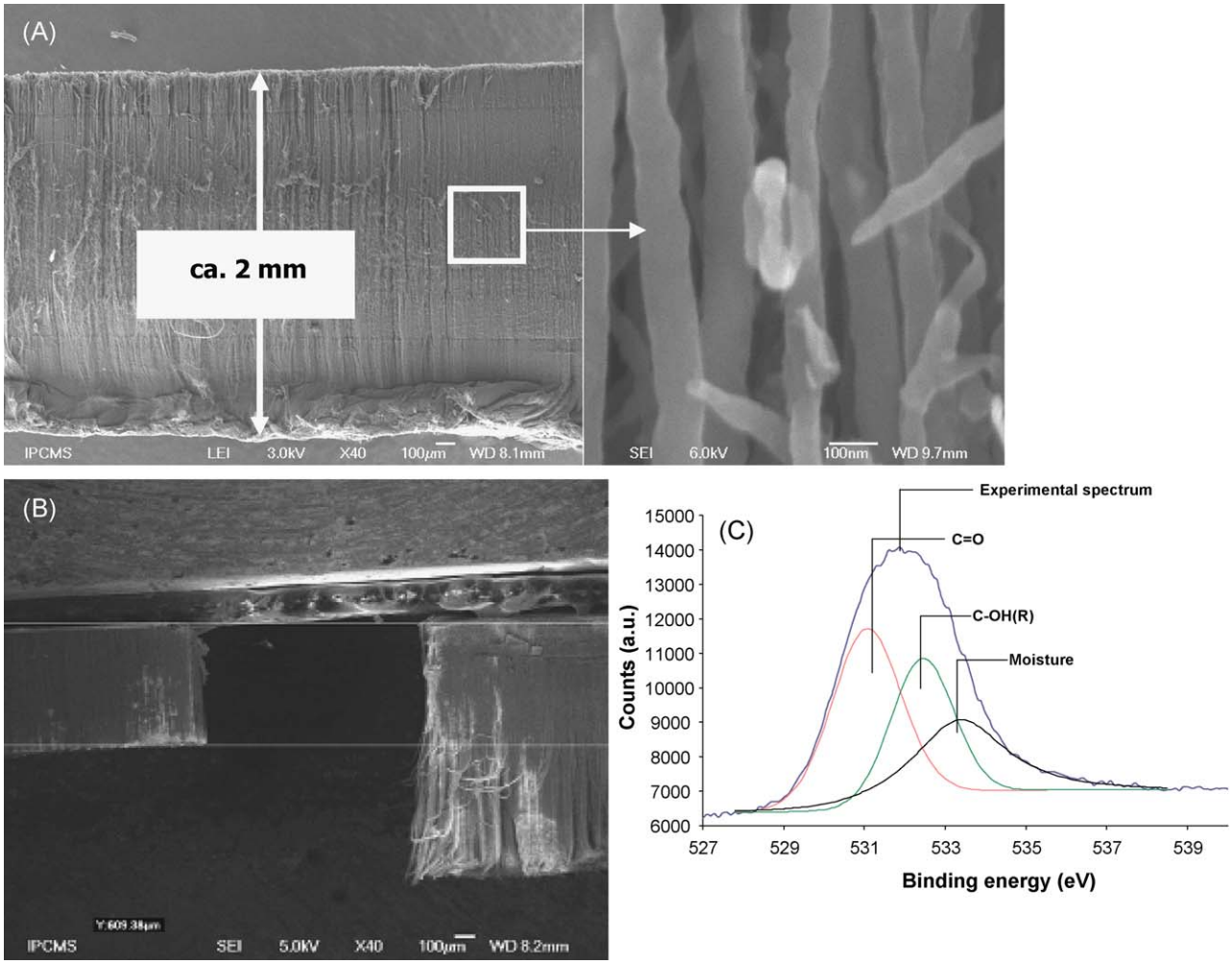

Fig. 2. (A) SEM micrograph of the VA-CNTs synthesized by CVD with a mixture of $Fe(C_5H_5)_2/C_7H_8$ at 850 °C for 2 h. *Inset*: high magnification SEM micrograph showing the homogeneous diameter of the nanotubes centered at ca. 100 nm. (B) SEM micrographs of the VA-CNTs as a function of the synthesis durations: left: 500 μm after 1 h of reaction, right: 1200 μm after 2 h of reaction. (C) XPS O_{1s} spectrum showing the presence of several oxygenated functional groups on the VA-CNT surface.

(Fig. 2A). Such diameter is slightly higher compared to the one typically reported for VA-CNTs obtained via the ferrocene method on quartz substrates which rang between 30–50 nm [25] and 60 nm [22,26]. We tentatively attribute this difference to the nature of the quartz substrate employed between these different syntheses. Indeed, the quartz substrate nature change could further alter the adhesion energy between the catalytic iron particles and the substrate which, in turn, modify the size of the iron catalyst. Similar change has also been observed on VA-CNTs obtained from ferrocene on a TiO_2 substrate [27].

It is noteworthy that the length of the VA-CNT carpet can be finely controlled by adjusting the synthesis duration (Fig. 2B), without changing the average diameter or alignment of the nanotubes. The SEM image (Fig. 2B) was obtained by fixing two VA-CNT samples, synthesized at different durations and removed from the substrate by a razor, on a graphite tape. SEM observations at medium resolution (not reported) clearly show the preferential orientation of the nanotubes perpendicularly with respect to the quartz substrate surface. SEM observations of the top of the carbon nanotube forest showed the absence of iron particles attached at the tube tip. The observed results were in good agreement with those reported by Resasco during the growth of vertical single-walled carbon nanotube array on silica substrate, who described a root growth mechanism in which the iron catalyst remained attached to the substrate surface while the nanotubes were slowly lift-off with an aligned morphology [28]. The as-synthesised VA-CNTs were took-off from the quartz substrate and treated in an acid solution maintained at 80 °C for 2 h in order to eliminate the residual catalyst and also to generate oxygenated functional groups on the surface [29]. It is worth mentioning, that the VA-CNT exhibits a high mechanical strength and thus, neither noticeable loss of carbon material nor macroscopic shape breaking were observed after the cleaning procedure. The presence of the oxygenated functional groups on the acid treated sample was followed by X-ray Photoelectron Spectroscopy (XPS) and the results are presented in Fig. 2C. According to the XPS results, the carbon nanotube surface is functionalized with several oxygenated functional groups. It is expected that these oxygenated groups will significantly alter the nature of the support surface, i.e. increase of the hydrophilic character, which favors the anchorage and dispersion of the active phase for the subsequent use of the material as catalyst support [30,31].

The specific surface area of the VA-CNTs measured by N_2 adsorption at liquid N_2 temperature was amounted to ca. 30 $m^2\,g^{-1}$ which is lower than the average value of random carbon nanotubes reported in the literature [32]. The relatively low surface area observed could be attributed to the high crystallinity of the material with low topological defects along the tube axis as observed by TEM. It is noteworthy that the specific surface area of the VA-CNTs is only linked to the external surface as no pores are present inside the material (see discussion below).

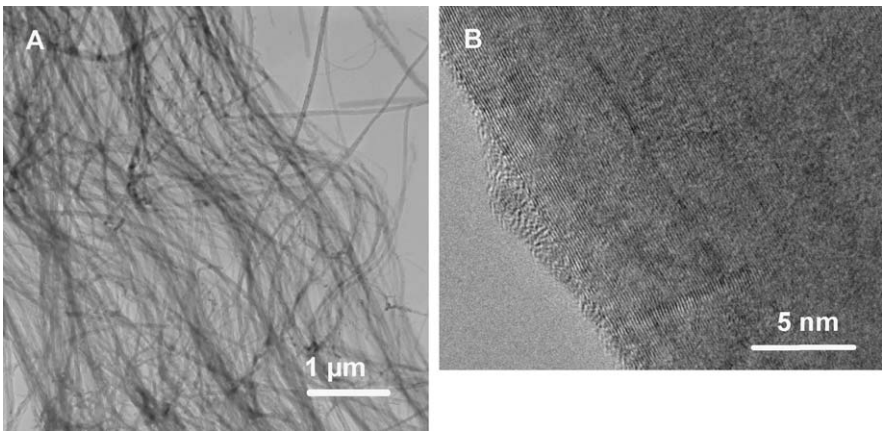

Fig. 3. TEM micrographs with different magnifications of the VA-CNT after acid washing.

The microstructure of the VA-CNTs was investigated by TEM and the results are presented in Fig. 3A and B. It is worth mentioning that along with straight tubes some curled tubes were also observed within the sample. For the moment, no clear mechanism has been advanced to explain such phenomenon. High-resolution TEM micrograph (Fig. 3B) indicates that the nanotubes walls are extremely well crystallized along the tube axis owing to the relatively high synthesis temperature. Indeed, previous results obtained on CNTs synthesized at lower temperatures show the presence of a relatively high amount of topological defects along the tube axis [33]. It was expected that at a higher synthesis temperature, the pentagone (negative curvature) or heptagone (positive curvature) insertion into the hexagone network was significantly lowered, thus, reducing the topological defects along the tube axis. The nature of the catalyst involved in the two synthesis processes, i.e. a homogeneous gas-phase feeding in the present work versus solid anchored catalyst particles in the classical CVD method, could also be responsible for such a difference.

It is noteworthy that the VA-CNTs possess a relatively narrow internal channel, i.e. 5 nm, compared to what is usually observed with random carbon nanotubes synthesized at lower reaction temperature, i.e. >10 nm. In addition, after synthesis, and unless specific treatment, most part of the nanotube channel was closed and thus, the inner channel pores are not available to the reactants and only inter-tube porosity should be considered during the catalytic test.

The complete removal of the iron catalyst is also evidenced by the SEM micrographs taken on the tube after synthesis and the one after acid treatment (Fig. 4).

TEM analysis also indicates the presence of some encapsulated iron-based compounds within the channel of the tube which were not removed during the post-synthesis acid treatment (Fig. 5). However, those iron nanorods are completely wrapped with graphene layers and thus, are no longer accessible to the reactants for further catalytic applications. Such encapsulated iron nanoparticles were already reported by Park and Keane [34] and by Anderson and Rodriguez [35]. This location resulted from the sucking of the starting iron catalyst inside the tube channel during its growth according to the results reported by Ermakova et al. [36]. The end-cap of the VA-CNTs also prevents any reaction within the tube channel. The oxidative behaviour of the carbon support was evaluated by TGA. According to the results, the VA-CNTs start to oxidize at a temperature well above the one obtained with the entangled carbon nanotubes formed on a Fe/Al_2O_3 catalyst at lower synthesis temperature, i.e. 760 °C instead of 680 °C. Such an oxidative temperature increase can be well correlated to the high crystallinity of the tube walls as observed by HR-TEM. The residual iron determined after the TGA is ca. 0.1 wt.%.

The assembly of the support and the platelet reactor is schematically represented in Fig. 6A. The platelet host reactor was made from a stainless steel plate with a single central channel (length × depth × width, 40 mm × 2 mm × 40 mm) with a large gas entrance and exit. The macroscopic dimension of the channel allows it to be machined by a traditional mechanical device without any need for complex technology as encountered with the

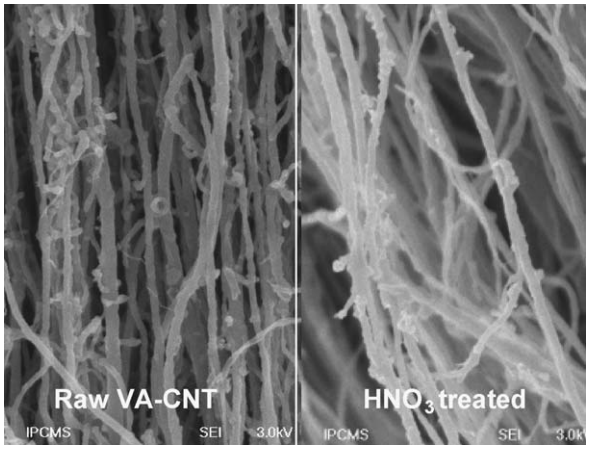

Fig. 4. SEM micrographs of the nanotubes after synthesis and after acid treatment showing the complete removal of the iron catalyst on the outer surface of the tubes.

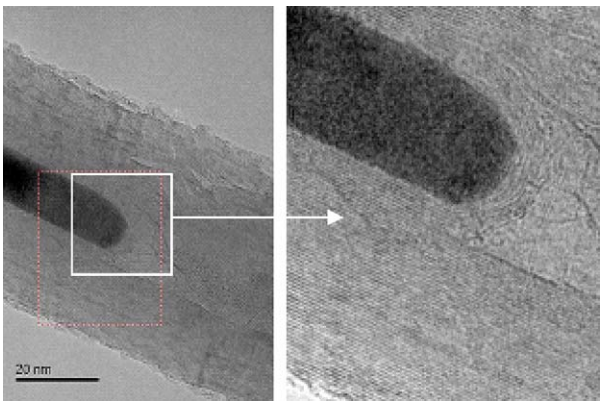

Fig. 5. Iron nanorod encapsulated by graphene layers (arrow) within the nanotube channel which was not removed by the acid treatment.

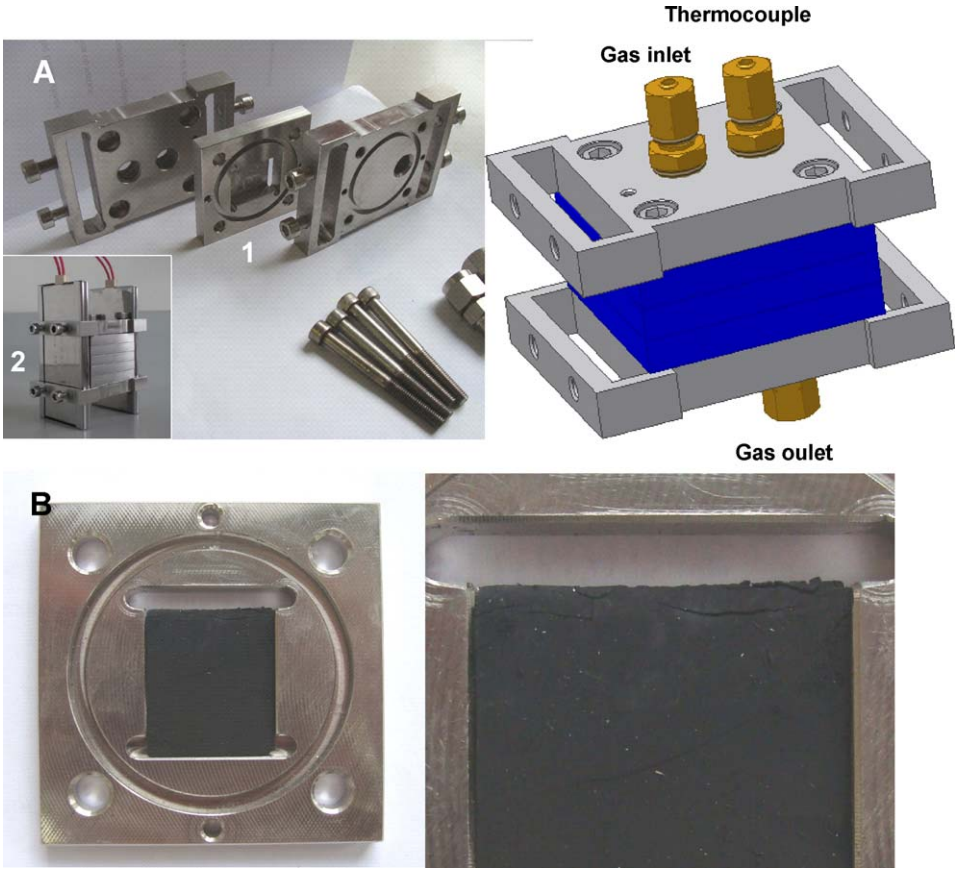

Fig. 6. (A) (Left) Platelet reactor structure and mode of assembly. (1) Reactor plate with a stainless-steel O-ring and the channel for catalyst localization. (2) Electrical plates allowing heat the reactor up to 500 °C. (Right) Schematic presentation of the reactor assembly with gas inlet and outlet and the thermocouple well. (B) Optical photos showing the assembly of the VA-CNTs inside the reactor chamber. In the closer-view photo (right) a crack is observed on the top part of the VA-CNTs due to the constraint during the drying process after the acid treatment. However, the crack is superficial and has no influence on the mechanical behaviour of the material. A quartz plate, 0.2 mm thick, was deposited on the top surface of the nanotubes carpet in order to avoid the problem of flow channelling in the free space between the nanotube carpet and the reactor upper plate.

microstructured reactors with sub-millimeter dimension. The plate of VA-CNTs (fitting the dimension of the reactor channel) was placed inside the channel. Obviously the height of the VA-CNTs does not perfectly fit with the height of the reactor channel, the height difference between the two systems is ca. 0.2 mm (10% of the maximum height of the reactor channel). In order to avoid the gas bypassing during the catalytic test a thin plate of quartz, 0.2 mm, was placed on the top of the VA-CNT carpet. We have assumed that the gas flow is randomly passing through the VA-CNTs structure taking into account the regular spacing between the carbon nanotube inside the carpet (see Fig. 2A). However, the liquid distribution within the platelet reactor filled with VA-CNTs is not fully understood yet. One should recall the fact that flow distribution, mass and heat transfers are still not clear for now in the case of the foam structures despite their longer use in microreactor system [37,38]. In the case of VA-CNTs filled channel, one cannot assume the complete absence of any channeling flow during the reaction.

However, results obtained on the liquid–liquid phase mixing carried out on hybrid reactors filled with different structures, i.e. VA-CNTs, felt and foam, have shown that the VA-CNTs is the most efficient structure for L–L mixing (Table 1). The high external surface area combines with the high tortuosity of the VA-CNT packed structure lead to an achievement of a high mixing degree between the two liquids resulting to a small droplet diameter compared to the other packed structures. It is expected that such nanoscopic packed structure could be efficiently employed as catalyst support in a liquid–liquid phase reaction where a high degree of mixing is a prerequisite. Work is ongoing to control the tube spacing, by controlling the catalyst, carbon source ratio and synthesis duration, in order to reduce as much as possible the problem of flow channelling through such nanoscopic material.

In order to compare the new hybrid platelet reactor in this work with the "classical" microreactor filled spherical particles, which represents the same pressure drop than the VA-CNT reactor (8.0×10^3 Pa m^{-1} for a linear space velocity of 0.04 m s^{-1}), we have used the Ergun equation to calculate the equivalent particle size of the material. According to the Ergun equation, the equivalent particle size of the fixed bed reactor having the same pressure drop is ca. 300 μm. It should also be noted that such "small" equivalent diameter is not unrealistic as one can find several literature reports using such particle size in fixed bed reactor [39–42]. The effective surface area of the platelet reactor filled with a carpet of VA-CNTs versus the unfilled one is significantly increased from 500 m^2 m^{-3} to 3×10^6 m^2 m^{-3} which highlight the effectiveness of the method (Table 2). The pressure

Table 1
Efficiency of the different structured materials in the hybrid platelet reactor for liquid–liquid phase mixing: water and toluene.

	Foam[a]	Felt[b]	VA-CNTs
Stabilisation time (s)	480	780	1440
Settling velocity (m s^{-1})	25×10^{-5}	15×10^{-5}	8×10^{-5}
Droplet diameter (μm)	60	47	35

[a] Foam structure with a strut diameter of 100 μm and a porosity of 91%.
[b] Felt structure with a microfilament diameter of ca. 10 μm and a porosity of 89%.

Table 2
Catalytic support characteristics and the influence of the support morphology on the effective specific surface area (contact surface) and pressure drop across the reactor channel.

Support characteristics	Empty platelet reactor	Spherical particles[a]	Carbon nanotubes[a]
Open porosity (ε)	1	0.40	0.91
Characteristic length of the material (μm)	–	$d_{particle} = 300$[a]	$d_{strut} = 100$
Effective specific surface area (a_c) ($m^2\,m^{-3}$)	500	12×10^3	3500×10^3
Pressure drop ($Pa\,m^{-1}$) at a linear velocity of $0.04\,m\,s^{-1}$	0	7.9×10^3	8.0×10^3

[a] The equivalent particle size chosen in this work is calculated from the Ergun equation in order to have a pressure drop similar as the one observed on the VA-CNT hybrid platelet reactor.

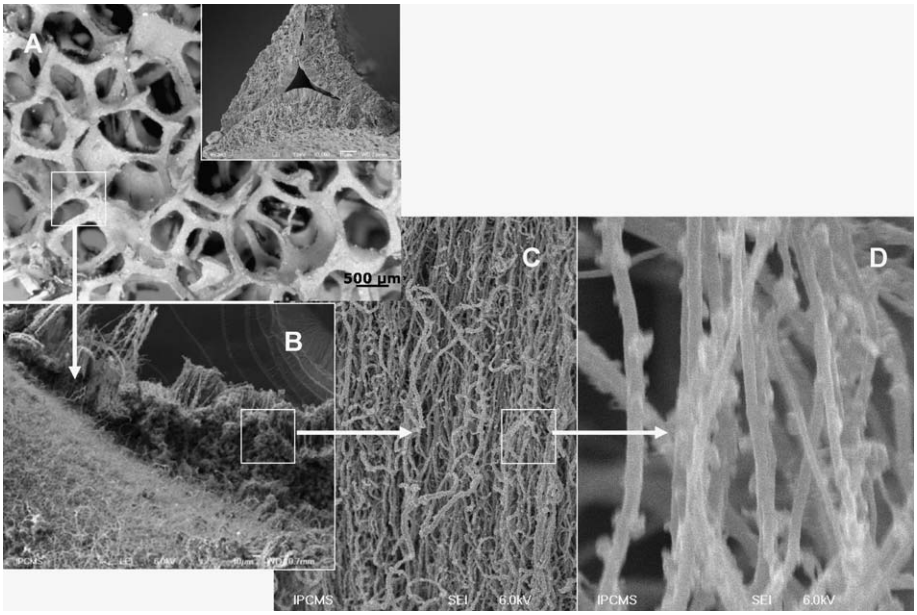

Fig. 7. SEM micrographs of the hierarchical support consisted by an array of vertically aligned carbon nanotubes on a SiC foam host structure.

drop across the reactor as a function of the gaseous space velocity is kept rather low and is comparable with a "packed-bed" type microreactor, filled with the spherical particles with an average diameter of 300 μm, i.e. 7.9×10^3 Pa m^{-1} instead of 8.0×10^3 Pa m^{-1}. The effective specific surface area is much higher in the case of VA-CNTs than the one filled with spherical particles, roughly three hundred times higher (Table 2).

It is worth mentioning that the difference in terms of the effective surface area between the VA-CNT bed and the spherical packed bed should be lower in reality. Indeed, in the present work the internal surface area of the spherical packed-bed is not taken into account and thus, one should expect a smaller difference in terms of effective surface area between the two systems. However, the high effective surface area of the VA-CNTs could find use in numerous reactions where high surface area linked to an internal porosity is not recommended, i.e. high space velocity gas-phase reaction where diffusional phenomenon could hinder or modify the catalytic activity or product selectivity: selective oxidation of traces of H_2S into elemental sulfur where pore diffusion could lead to a loss of sulfur selectivity towards the SO_2 formation, Fischer–Tropsch synthesis where the catalytic activity could be hindered due to problems of pore plugging by the liquid product. The same drawbacks also occur in the gas–liquid and/or liquid–liquid phase reactions where diffusion problems should be solved in order to maintain the activity and selectivity.

It is also noteworthy that the hybrid reactor described above can be filled not only with VA-CNTs but also with various structured materials such as carbon felt, carbon foam, SiC foam [43] either as such or decorated with a network of carbon or SiC nanofibers [44] depending on the downstream applications, i.e. liquid–liquid–solid (L–L–S), gas–liquid–solid (G–L–S) or gas–gas–solid (G–G–S) processes. Some examples of such hierarchical catalyst supports are presented in Fig. 7. Again, these hybrid materials show high mass and heat transfers compared to the conventional packed-bed reactor along with extremely low pressure drops [44].

4. Conclusion

In conclusion, a new hybrid platelet reactor filled with a carpet of catalytically grown VA-CNTs can be effectively produced and assembled as a LEGO®-like device. Due to the nanoscopic size of the filling material such reactor displays an extremely high surface-to-volume ratio, expressed in terms of effective surface area along with an affordable pressure drop across the reactor. The high S/V ratio and the complete volume filling ensure a high surface contact between the reactants and the catalyst while, contrary to the conventional microreactor reactor system, the possibility to remove the catalyst allows the easy control (preparation and characterizations) and replacement of the catalyst in case of deactivation or plugging represent a great advantage. The lack of internal porosity in this kind of support also provide new route for some severe reactions where diffusion induces a detrimental activity and selectivity loss. These nanoscopic catalyst support can be also grafted on another macroscopic host structure, i.e. felt or foam, which allows the reduction of the overall pressure drop on one hand, and provides a high contact surface with the reactant on the other hand. Catalytic evaluation work dealing with the gas–liquid selective C=C bond hydrogenation and Fischer–Tropsch synthesis in this kind of platelet nanoscopic reactor is ongoing and will be published soon.

Acknowledgements

TEM experiments were carried out at the IPCMS facilities. M. Houllé is gratefully acknowledged for help during the manuscript correction. Cacao J.P. is gratefully acknowledged for helpful stimulation during the work.

References

[1] K. Jähnisch, V. Hessel, H. Löwe, M. Baerns, Angew. Chem. Int. Ed. 43 (2004) 406 (and references therein).
[2] L. Kiwi-Minsker, A. Renken, Catal. Today 110 (2005) 2 (and references therein).
[3] K.P. Jäckel, in: W. Ehrfeld (Ed.), Microsystem Technology for Chemical and Biologicam Microreactors, DECHEMA Monographs, vol. 132, VCH, Weinheim, 1996, p. 29.
[4] T. Kawaguchi, H. Miyata, K. Ataka, K. Mae, J. Yoshida, Angew. Chem. Int. Ed. 44 (2005) 2413.
[5] I.Z. Ismagilov, E.M. Michurin, O.B. Sukhova, L.T. Tsykoza, E.V. Matus, M.A. Kerzhentsev, Z.R. Ismagilov, A.N. Zagoruiko, E.V. Rebrov, M.H.J.M. de Croon, J.C. Shouten, Chem. Eng. J. 135S (2008) S57.
[6] M. Crespo-Quesada, M. Grasemann, N. Semagina, A. Renken, L. Kiwi-Minsker, Catal. Today 147 (2009) 247.
[7] N. Semagina, et al. J. Catal. 251 (2007) 213.
[8] L. Pingle, L. Lefferts, Chin. J. Chem. Eng. 14 (2006) 294.
[9] N.A. Jarrah, J.G. van Ommen, L. Lefferts, J. Catal. 239 (2006) 460.
[10] Ph. Serp, M. Corrias, Ph. Kalck, Appl. Catal. A: Gen. 253 (2003) 337 (and references therein).
[11] C. Pham-Huu, O. Ersen, M.J. Ledoux, Carbon and silicon carbide nanotubes containing catalysts, in: D. Astruc (Ed.), Nanoparticles and Catalysis, Wiley-VCH, Weinheim, 2008, p. 219 (and references therein).
[12] P.M. Ajayan, Chem. Rev. 99 (1999) 1787 (and references therein).
[13] W. Xia, O.F.K. Schlüter, C. Liang, M.W.E. van den Berg, M. Guraya, M. Muhler, Catal. Today 102–103 (2005) 34.
[14] J. Amadou, K. Chirazi, M. Houllé, I. Janowska, O. Ersen, D. Bégin, C. Pham-Huu, Catal. Today 138 (2008) 62.
[15] A. Caillard, C. Charles, R. Boswell, P. Brault, C. Coutanceau, Appl. Phys. Lett. 90 (2007) 223119.
[16] J. Jang, D.J. Liu, Carbon 45 (2007) 2843.
[17] G. Centi, S. Perathoner, Catal. Today 148 (2009) 191.
[18] I. Janowska, K. Chizari, J.H. Olivier, R. Ziessel, C. Pham-Huu, Adv. Synth. Catal., submitted for publication.
[19] C. Pham-Huu, I. Janowska, D. Edouard, V. Keller-Spitzer, N. Keller, M.J. Ledoux, French Pat. Appl. (2007), 07-08411.
[20] N. Ishigami, H. Ago, Y. Motoyama, M. Takasaki, M. Shinagawa, K. Takahashi, T. Ikuta, M. Tsuji, Chem. Commun. (2007) 1626.
[21] M. Pinault, V. Pichot, H. Khodja, P. Launois, C. Reynaud, M. Mayne-L'Hermite, Nano Lett. 5 (2005) 2394.
[22] I. Janowska, G. Winé, M.J. Ledoux, C. Pham-Huu, J. Mol. Catal. A: Chem. 267 (2007) 92.
[23] C. Singh, M.S.P. Schaffer, A.H. Windle, Carbon 41 (2003) 359.
[24] X. Li, A. Cao, Y.J. Jung, R. Vajtai, P.M. Ayajan, Nano Lett. 5 (2005) 1997.
[25] Z.J. Zhang, B.Q. Wei, G. Ramanath, P.M. Ajayan, Appl. Phys. Lett. 77 (2000) 3764.
[26] I. Janowska, S. Hajiesmaili, D. Bégin, V. Keller, N. Keller, M.J. Ledoux, C. Pham-Huu, Catal. Today 145 (2009) 76.
[27] P. Ruvinsky, A. Bonnefont, M. Houllé, C. Pham-Huu, E.R. Savinova, Electrochem. Acta, submitted for publication.
[28] L. Zhang, Y. Tan, D.E. Resasco, Chem. Phys. Lett. 422 (2006) 198.
[29] P.C.P. Watts, N. Mureau, Z. Tang, Y. Miyajima, J.D. Carey, S.R.P. Silva, Nanotechnology 18 (2007) 175701.
[30] C. Pham-Huu, M.J. Ledoux, Top. Catal. 40 (2006) 49.
[31] W. Li, C. Liang, W. Zhou, J. Qiu, G. Sun, Q. Xin, J. Phys. Chem. B 107 (2003) 6292.
[32] K. Dasgupta, S. Kar, R. Venugopalan, R.C. Bindal, S. Prabhakar, P.K. Tewari, S. Bhattacharya, S.K. Gupta, D. Sathiyamoorthy, Mater. Lett. 62 (2008) 1989.
[33] J. Amadou, D. Bégin, P. Nguyen, J.P. Tessonnier, Th. Dintzer, E. Vanhaecke, M.J. Ledoux, C. Pham-Huu, Carbon 44 (2006) 2587.
[34] C. Park, M.A. Keane, Langmuir 17 (2001) 8386.
[35] P.E. Anderson, N.M. Rodriguez, Chem. Mater. 12 (2000) 823.
[36] M.A. Ermakova, D.Y. Ermakov, A.L. Chuvilin, G.G. Kuvshinov, J. Catal. 201 (2001) 183.
[37] D. Edouard, M. Lacroix, C. Pham-Huu, F. Luck, Chem. Eng. J. 144 (2008) 289.
[38] D. Edouard, M. Lacroix, Ch. Pham, M. Mbodji, C. Pham-Huu, AIChE J. 54 (2008) 2823.
[39] S.R. Deshmukh, A.B. Mhadeshwae, D.G. Vlachos, Ind. Eng. Chem. Res. 43 (2004) 2986.
[40] S. Jam, M.G. Ahangary, A. Tavasoli, K. Sadaghiani, A.N. Pour, React. Kinet. Catal. Lett. 89 (2006) 71.
[41] C. Cao, D.R. Palo, A.L.Y. Tonkovich, Y. Wang, Catal. Today 125 (2007) 29.
[42] Website: www.velocys.com (and references therein).
[43] www.sicatcatalyst.com.
[44] E. Vanhaecke, S. Ivanova, O. Ersen, A. Deneuve, D. Edouard, G. Winé, P. Nguyen, Ch. Pham, C. Pham-Huu, J. Mater. Chem. 18 (2008) 4654.